24th INTERNATIONAL CONGRESS ON SOUND AND VIBRATION
23–27 July 2017, London

DECENTRALISED ACTIVE VIBRATION CONTROL USING A REMOTE SENSING STRATEGY

Joseph Milton
University of Southampton, Faculty of Engineering and the Environment, Highfield, Southampton, UK
email: jm3g13@soton.ac.uk

Jordan Cheer
University of Southampton, Faculty of Engineering and the Environment, Highfield, Southampton, UK

Steve Daley
University of Southampton, Faculty of Engineering and the Environment, Highfield, Southampton, UK

In many applications it is desirable to use a decentralised control strategy, in which multiple sensor-actuator pairs are utilised to control the response of a structure. This avoids the need for connections between multiple sensors and actuators and allows the system to be easily scaled to different applications. However, because the individual control loops, consisting of a single sensor-actuator pair, only have a direct measurement of the local vibration signal it is not straightforward to guarantee global reduction of the kinetic energy of the structure. In this paper a novel decentralised control strategy is proposed in which the vibration at remote locations is estimated utilising the local error sensor signal and the local control loop is then adapted to minimise the sum of both the squared local and the estimated remote error signals. When multiple loops are employed, it is also necessary for each local control loop to predict the global effect of the remote control signals and use this information in the adaptation of the local control loop. This paper describes the proposed control strategy, including the calibration of the algorithm and the estimation of the error and control signals. The proposed control strategy is evaluated through simulation of an acoustically excited flat panel and its performance is compared to both standard centralised and decentralised control strategies.

Keywords: active vibration control, decentralised control, remote sensing.

1. Introduction

Active vibration control (AVC) can be used as a versatile way to reduce the vibration of an excited structure. AVC provides the potential for a much greater level of control compared to passive methods, especially when size and weight criteria must be met [1]. Using AVC it is possible to flexibly manipulate the structural and acoustic response of a system such that control can be achieved at a selected frequency and adapted if required.

In general, AVC can be implemented in two ways, using either a centralised or decentralised architecture. In a centralised control system, an array of connected error sensors are used to detect the vibration on a structure and a control system is then used to manipulate the measured signals and drive an array of control actuators to reduce the measured vibrations. In a decentralised control system, pairs of collocated sensors and actuators are used to measure the vibration on a structure locally and a local controller is then used to manipulate the measured signal and drive the actuator to control the measured vibration [1]. Both the centralised and decentralised approaches have advantages

and disadvantages and depending on the design criteria one approach may be more suited to a specific application than the other. For example, a decentralised system may be better suited to applications where it is important to avoid large amounts of cabling between the different parts of the control system and where the scalability of the control design is important. However, because a decentralised AVC system only has access to a local measurement of the vibration, it is not straightforward to guarantee global control of the structural response. Decentralised controllers are typically unaware of the effect they have on the response of a structure at remote locations or the combined effects that occur when multiple controllers are implemented. Centralised controllers on the other hand take into account the cross coupling between units and work as one to minimise a global cost function, the disadvantages of centralised control however, are that for larger structures that require more actuators, considerable amounts of cabling would be required, adding to the overall weight of the system and an increased installation cost.

To over-come the obstacles presented by standard centralised and decentralised active vibration control strategies, this paper will combine a remote sensing method and a decentralised active vibration control approach to design a control system that is decentralised, but able to control the global response of the structure. The proposed decentralised remote sensing control strategy does not require real time communication between the control units, but instead each local control loop estimates the error signals at the remote locations and generates a local control signal that assumes coordinated control at the remote controller positions. In order to assess the performance of this control strategy, centralised and decentralised control systems were initially implemented to provide a reference for the performance of the decentralised remote sensing controller.

2. Formulation of decentralised active vibration control using a remote sensing strategy

2.1 Active vibration control

The following mathematical formulation is for a centralised Multi-input Multi-Output (MIMO) system operating at a single frequency. The aim of AVC in this case is to minimise the sum of the squared signals measured at the L error sensors, this can be defined at a single frequency by the following cost function.

$$J_s = \mathbf{e}^H \mathbf{e}, \tag{1}$$

where $\mathbf{e}$ is the vector of L error signals in the steady state measured on the surface of the panel, $\mathbf{e} = [e_1\ e_2\ ...\ e_L]^T$. This is given by the linear superposition of the primary disturbance measured at the error sensors, $\mathbf{d}$, and the contribution due to the controller, $\mathbf{Gu}$. For a centralised system, the following equation can then be used to calculate $\mathbf{e}$,

$$\mathbf{e} = \mathbf{d} + \mathbf{Gu}, \tag{2}$$

where $\mathbf{d}$ is the $(L \times 1)$ vector of the primary disturbances at the error sensor locations, $\mathbf{G}$ is the $(L \times M)$ matrix of transfer responses between the input to the structural control actuators and the resulting, L, accelerations measured at the error sensor locations and $\mathbf{u}$ is the $(M \times 1)$ vector of control signals used to control the response of the structure. Substituting eqn.2 into eqn.1 gives the cost function as

$$J_s = \mathbf{u}^H \mathbf{G}^H \mathbf{G}\mathbf{u} + \mathbf{d}^H \mathbf{G}\mathbf{u} + \mathbf{u}^H \mathbf{G}^H \mathbf{d} + \mathbf{d}^H \mathbf{d}. \tag{3}$$

If the matrix $\mathbf{G}^H\mathbf{G}$ is assumed to be positive definite, which is generally the case [2], then the control signals that minimise J_s are generated by setting the derivative of eqn.3 with respect to the real and imaginary parts of $\mathbf{u}$ to zero. The optimal vector of control signals is then

$$\mathbf{u}_{opt} = -[\mathbf{G}^H \mathbf{G}]^{-1} \mathbf{G}\mathbf{d}, \tag{4}$$

If $L = M$, which is the case for the decentralised controller, then the optimal vector of control signals becomes

$$\mathbf{u}_{opt} = -\mathbf{G}^{-1}\mathbf{d}. \tag{5}$$

In practical applications the disturbance signals are not known in advance and therefore, to minimise the sum of squared error signals in realtime, an algorithm able to iteratively adjust the input to the control actuators, $\mathbf{u}$, is needed. The method of steepest decent was used to manipulate the measured signals and drive the control actuators to alter the response of the structure in such to way so as to minimise the measured error signals. The steepest decent update algorithm that was used was

$$\mathbf{u}(n+1) = \gamma\mathbf{u}(n) - \alpha\mathbf{G}^{H}\mathbf{e}, \tag{6}$$

where n represents the current iteration step of the algorithm, γ is the leakage factor and α is the convergence gain. Simulation of the decentralised system uses the same mathematical formulation, however, the plant matrix $\mathbf{G}$ contains only transfer responses between local actuator-sensor pairs.

2.2 Decentralised remote sensing active vibration control

In the case of a decentralised controller, since there are no connections between the local control loops, it is not straightforward to minimise the sum of the squared error signals given by eqn. 1. To attempt to overcome this problem, it is proposed here to use a remote sensing strategy algorithm to estimate the error signals at the remote sensors from the local measured error signal. Remote sensing strategies have been employed in active noise control systems and vibration control systems to estimate the pressures and structural responses at locations that cannot be directly measured [3, 4, 5, 6, 7, 8], however, they have not previously been integrated into a decentralised control framework. The distinction in this case is that it is necessary to estimate both the remote error signals and the effect of the remote control actuators.

Assuming perfect knowledge of the plant response matrix, the estimated remote error signals for the l^{th} control loop can be expressed as

$$\hat{\mathbf{e}}_l = \hat{\mathbf{d}}_l + \mathbf{G}\hat{\mathbf{u}}_l, \tag{7}$$

where $\hat{\mathbf{d}}_l$ is the vector of primary signals estimated at the remote locations, $\mathbf{G}$ is the $(L \times L)$ plant response matrix, and $\hat{\mathbf{u}}_l$ is the vector of estimated control signals.

The primary disturbance at the remote error sensors can be estimated for the l^{th} control loop from the single local measured signal as a linear function of an observation filter, $\mathbf{O}_l$,

$$\hat{\mathbf{d}}_l = \mathbf{O}_l\hat{d}_l, \tag{8}$$

where $\hat{d}_l$ is the estimate of the primary disturbance at the local error sensor, which can be expressed in terms of the local error signal e_l, the $(1 \times L)$ vector of responses from each actuator to the local error sensor, $\mathbf{g}_l$, and the $(L \times 1)$ vector of estimated control signals $\hat{\mathbf{u}}_l$.

$$\hat{d}_l = e_l - \mathbf{g}_l\hat{\mathbf{u}}_l. \tag{9}$$

The optimal observation filter for the l^{th} control loop, $\mathbf{O}_{l,opt}$ can be calculated by minimising the cost function

$$J_O = \text{trace}[(\mathbf{d} - \mathbf{O}\hat{d}_l)(\mathbf{d}^H - \hat{d}_l^*\mathbf{O}_l^H)]. \tag{10}$$

where * denotes the complex conjugate. The matrix of optimum observation filters for the l^{th} control loop is then [9]

$$\mathbf{O}_{l,opt} = \frac{\mathbf{d}\hat{d}_l^*}{\hat{d}_l\hat{d}_l^*} = \frac{\mathbf{d}}{\hat{d}_l}, \tag{11}$$

The cost function given by the sum of the squared estimated error signals for the l^{th} control loop can then be expressed as

$$J_l = \hat{\mathbf{e}}_l^H \hat{\mathbf{e}}_l. \tag{12}$$

Substituting in eqn.7 and 8 the cost function can then be written as

$$J_l = (\hat{d}_l^* \mathbf{O}_l^H + \hat{\mathbf{u}}_l^H \mathbf{G}^H)(\mathbf{O}_l \hat{d}_l + \mathbf{G}\hat{\mathbf{u}}_l). \tag{13}$$

From this, the vector of optimal control signals for the l^{th} loop can be calculated as

$$\hat{\mathbf{u}}_{l,opt} = -\mathbf{G}^{-1}\mathbf{O}_l \hat{d}_l, \tag{14}$$

which will be equivalent to 5 provided the observation filter provides a perfect estimation of the remote signals.

As in the case of the MIMO centralised controller described in Section 2.1, it is generally necessary to iteratively calculate the control signals.This can be achieved by using the steepest-decent algorithm and for the l^{th} control loop using the remote sensor method the update equation is given by

$$\hat{\mathbf{u}}_l(n+1) = \gamma \hat{\mathbf{u}}_l(n) - \alpha \mathbf{G}^H \hat{\mathbf{e}}_l. \tag{15}$$

Substituting in eqn.7 for the estimated error signals and using the estimated disturbance, given by eqn.8 and eqn.9, the update algorithm for the l^{th} control signal becomes

$$\hat{\mathbf{u}}_l(n+1) = [\gamma \mathbf{I} - \alpha \mathbf{G}^H \mathbf{G} + \alpha \mathbf{G}^H \mathbf{O}_l \mathbf{g}_l]\hat{\mathbf{u}}_l(n) - \alpha \mathbf{G}^H \mathbf{O}_l e_l(n). \tag{16}$$

The decentralised remote sensing controller with L control loops can then be implemented by using the update equation given in eqn.16 at each of the individual local control loops.

3. Performance assessment

The performance of the three control strategies were assessed through simulations using the responses measured for a (4×4) AVC system mounted to a flat aluminium panel, as shown in Fig.1.

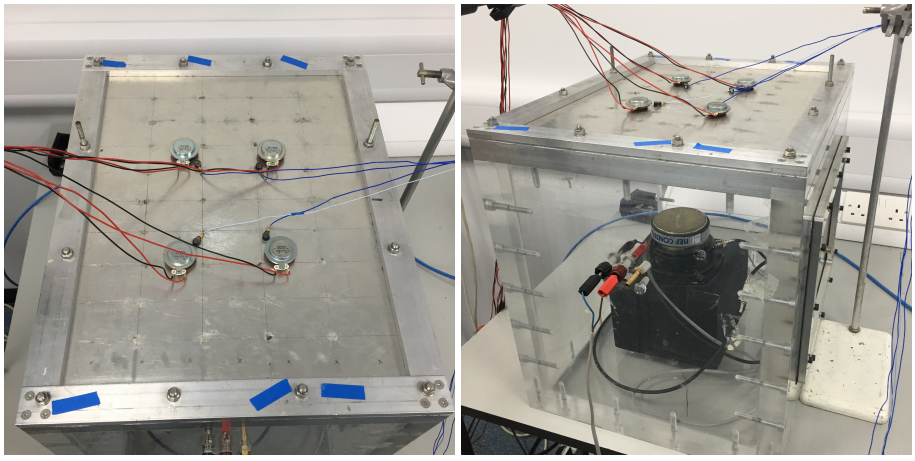

(a) (b)

Figure 1: *Photographs of the accelerometer and actuator arrangement (a) and the panel mounted on the enclosure containing the primary disturbance loudspeaker (b).*

Each of the four actuators shown in Fig.1a were driven separately with white noise and the transfer responses between each actuator and accelerometer were then calculated and used to form the plant

model. The primary disturbance was provided by the loudspeaker shown in Fig.1b and this was also driven with white noise in order to excite the panel and generate the primary response models.

The mathematical formulation of the control systems derived in section 2 assumes that the error signals have reached their steady state values before the control signals are updated [2]. In this preliminary study the simulations have been implemented in the frequency domain so that all signals are steady state. However, in practice difficulties can occur because transients may not have have decayed away before the control signals are updated and in this case the steady state assumption will be violated. Decentralised remote sensing AVC appears to be more sensitive to this steady state assumption due to the complex nature of the control formulation leading to a compounding of the errors. A possible solution to overcome this issue is to implement a decentralised remote sensing AVC system that allows the error signals to reach the steady state before updating the controller.

3.1 Simulation study

To assess the feasibility of the decentralised remote sensing AVC strategy simulations for centralised, decentralised and decentralised remote sensing AVC were carried out at three selected frequencies. The frequencies selected were; 90.3, 122.1 and 190.4 Hz representing the breathing mode of the panel, an off resonance frequency and the second mode of the panel respectively. Fig 2 shows the magnitude and phase plots of the primary and plant responses of the panel.

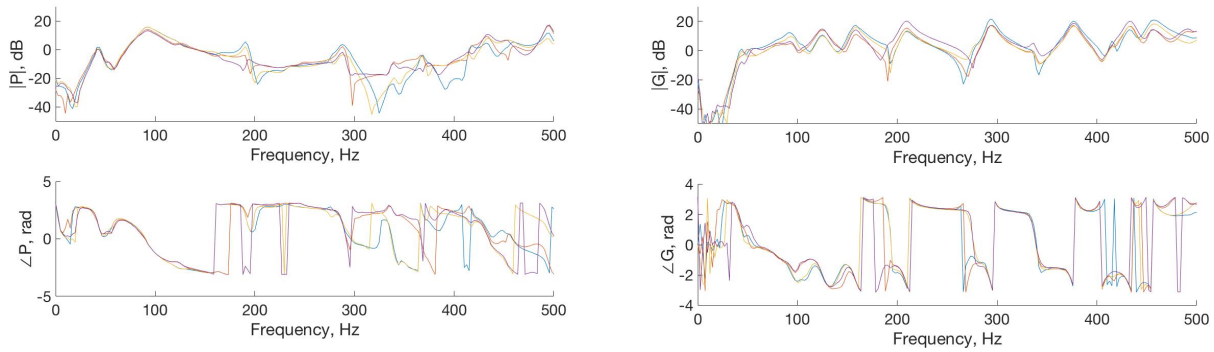

(a) *Primary response* (b) *Plant response*

Figure 2: *Magnitude and phase plot of the primary and plant responses measure on across the surface of the panel.*

Fig. 3 shows the convergence of the cost function, J_s for each system at the three frequencies. In each plot the black solid line represents centralised AVC, the blue solid line represents decentralised AVC and the red dashed line represents decentralised remote sensing AVC. The convergence gain and leakage for the active vibration control systems have been set to achieve the the quickest convergence time whilst maintaining a stable system.

Control at the 90 Hz breathing mode for all control systems shows the largest reduction in the overall response with the quickest convergence. Both centralised AVC and decentralised remote sensing AVC achieve approximately 20 dB reduction and decentralised AVC achieves a reduction of approximately 11 dB. Off resonance at 122 Hz the convergence time for all three control systems slows to maintain stability. The reduction of the overall response of the system is approximately 14 dB for both centralised AVC and decentralised remote sensing AVC and decentralised AVC shows a reduction of approximately 7dB. At the second mode, the performance of the systems is reduced further. Decentralised AVC is unable to reduce the response of the structure at all and both centralised AVC and decentralised remote sensing AVC achieve a maximum reduction of approximately 12 dB. Fig. 3 clearly shows that at all frequencies, the control curves for centralised AVC and decentralised remote sensing AVC are identical proving the validity of the mathematical formulation.

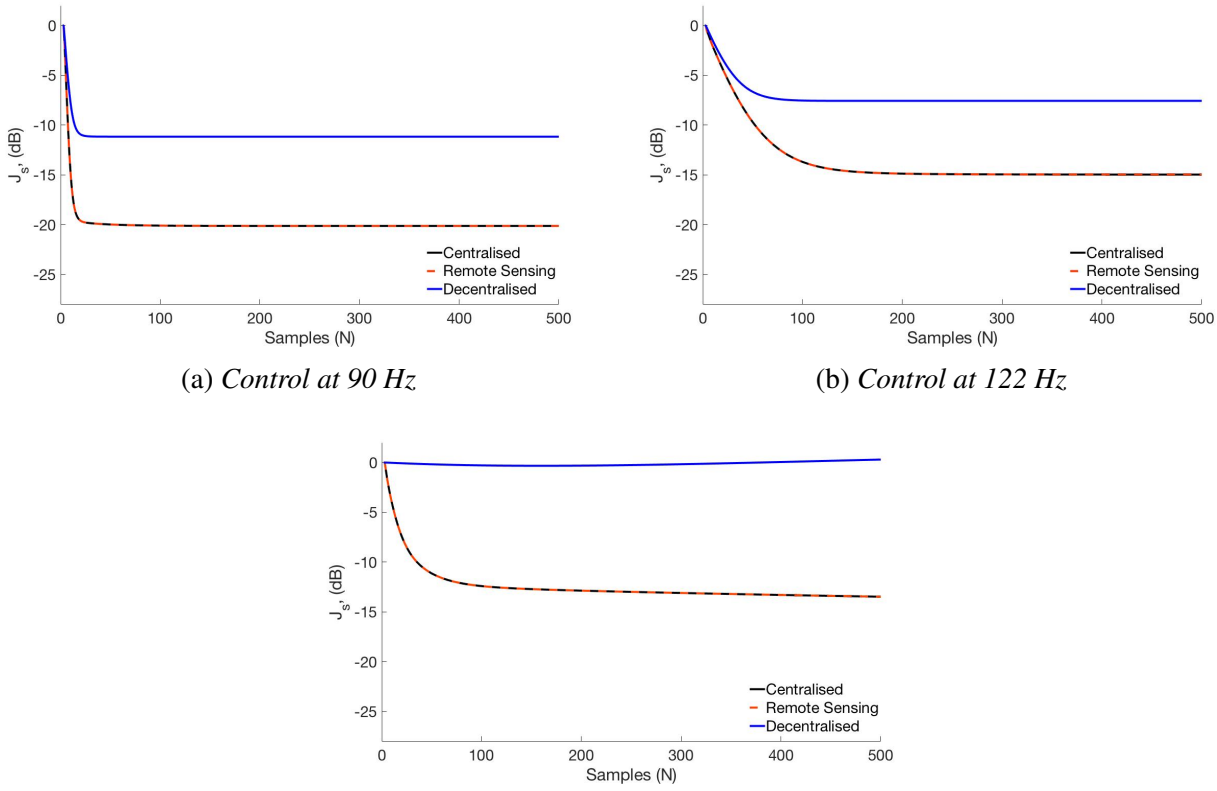

(a) *Control at 90 Hz*

(b) *Control at 122 Hz*

(c) *Control at 190 Hz*

Figure 3: *The convergence of the cost function J_s at each control frequency using the three control strategies.*

For a practical system, it is unlikely that estimated signals will perfectly match the physical signals due to changes in operating conditions introducing differences between the physical and modelled primary and plant responses. This would introduce a degree of uncertainty into the controller and this could affect the stability of the system.

In order to assess the sensitivity of the controllers to such uncertainties in the plant response, errors were introduced into the physical plant response matrix, $\mathbf{G}$ in eqn.2 and 7, as

$$\mathbf{G} = \mathbf{G}_0 + \Delta, \tag{17}$$

where $\mathbf{G}_0$ is the nominal plant response used in the controllers and Δ represents the error which has been defined as

$$\Delta = \epsilon^2 \frac{\mathrm{rand}(\mathrm{size}(\mathbf{G}))}{||G||_F} \tag{18}$$

where ϵ is set to 0.01 to evaluate the performance of the system when an error of 1% is present between the measured error signals and the plant models.

Fig. 4 shows the convergence of the cost function J_s for the three control strategies at each frequency. Leakage has been applied to each of the control systems to ensure that the system is stable after the addition of the plant response errors and, therefore, rather than assessing the stability directly the performance limit due to ensuring robust stability has been assessed.

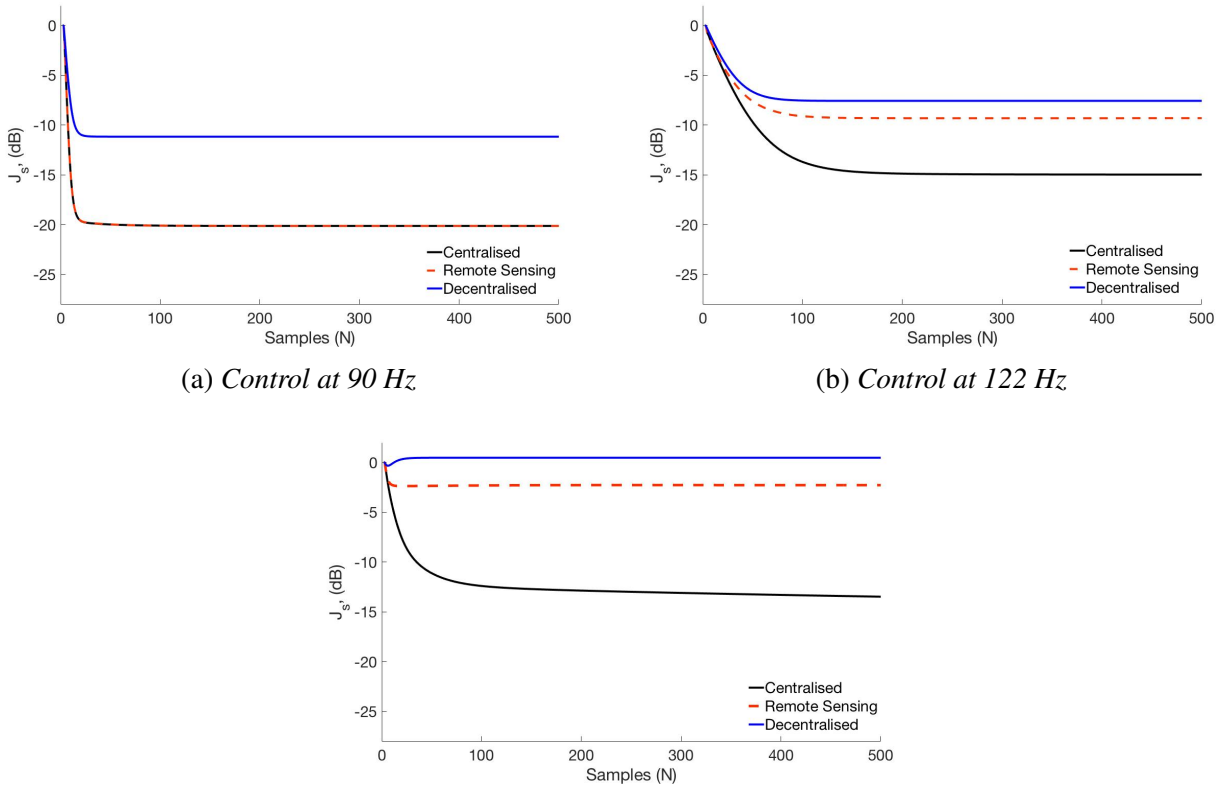

(a) *Control at 90 Hz*

(b) *Control at 122 Hz*

(c) *Control at 190 Hz*

Figure 4: *The convergence of the cost function J_s at each control frequency using the three control strategies when an artificial error of 1% is introduced into the plant response.*

As in Fig. 3, the black solid line represents centralised AVC, the blue solid line represents decentralised AVC and the red dashed line represents decentralised remote sensing AVC. With errors added to the physical plant response, control at 90 Hz is unaffected for all of the control strategies. To maintain robust stability at the off resonance frequency with the addition of plant response errors, an increase in leakage was required. As a result, the performance of the decentralised remote sensing system decreased by approximately 7 dB, however, the new method still out performed standard decentralised control by approximately 2 dB. For control at 190 Hz only the centralised control system is unaffected by the addition errors, the decentralised and decentralised remote sensing active vibration control systems both suffer a loss in performance in order maintain robust stability. Decentralised AVC at this frequency actually causes a small amplification in vibration whilst the performance of decentralised remote sensing AVC drops from a 12 dB reduction to 2 dB.

4. Conclusions

A new approach to designing a decentralised active vibration control system using a remote sensing strategy has been proposes in this paper. This approach avoids the need for a physical, real-time connection between controllers, whilst providing a comparable level of control to that of centralised AVC in a perfect simulation scenario.

It has been shown in simulation that under ideal conditions a decentralised remote sensing AVC system performs as well as centralised AVC. At frequencies above resonance the performance drops when a small error is introduced into the plant response, however, despite this reduction in performance when simulated errors are added, decentralised remote sensing AVC remains more effective than standard decentralised AVC.

Acknowledgments

This research is jointly funded by an EPSRC industrial CASE studentship and BAE systems.

REFERENCES

1. Fuller, C., Elliott, S. and Nelson, P., *Active control of vibration*, Academic Press London (1996).

2. Elliott, S. J., *Signal Processing for Active Control*, Academic Press London (2000).

3. Moreau, D., Cazzolato, B., Zander, B. and Petersen, C. A review of virtual sensing algorithms for active noise control, *Algorithms 1*, pp. 69–99, (2008).

4. Garcis-Bonito, J., Elliott, S. and Boucher, C. Generation of zones of quiet using a virtual microphone arrangement, *The Journal of the Acoustical Society of America*, **101** (2), 3498–3516, (1997).

5. Roure, A. and Albarrazin, A. The remote microphone technique for active noise control, *in Proceedings of the 1999 International Symposium on Active Control of Sound and Vibration (Active 99)*, pp. 1233–1244, (1999).

6. Elliott, S. and Cheer, J. Modeling local active sound control with remote sensors in spatially random pressure fields, *The Journal of the Acoustical Society of America*, **137** (4), 1936–1946, (2015).

7. Wang, J. and Daley, S. Broadband controller design for remote vibration using a geometric approach, *Journal of Sound and Vibration*, **329** (19), 3888–3897, (2010).

8. Ubaid, U., Daley, S. and Pope, S. Design of remotely located and multi-loop vibration controllers using a sequential loop closing approach, *Control Engineering Practice*, **38**, 1–10, (2015).

9. Elliott, S. and Cheer, J. Modelling local active sound control with remote sensors in spatially random pressure fields, *The Journal of the Acoustical Society of America*, **137** (4), 1936–1946, (2015).